Measurement of the angular correlation parameters in the β decay of polarized Λ hyperons*

J. Lindquist,† E. C. Swallow,‡ R. L. Sumner,§ J. M. Watson,‖ R. Winston,¶ and D. M. Wolfe**
Enrico Fermi Institute, The University of Chicago, Chicago, Illinois 60637

K. Reibel, D. M. Schwartz,†† and A. J. Stevens‡‡
Ohio State University, Columbus, Ohio 43210

T. A. Romanowski
Argonne National Laboratory, Argonne, Illinois 60439
and Ohio State University, Columbus, Ohio 43210

(Received 28 October 1975; revised manuscript received 23 May 1977)

We present our final results from an experimental investigation of the β decay of polarized Λ hyperons with a large-aperture magnetic spectrometer. Our data sample consists of 544 events. We obtain $A_\nu = 0.72 \pm 0.12$, $A_e = 0.05 \pm 0.12$, and $A_p = -0.47 \pm 0.12$ for the three spin-asymmetry parameters, and $A_{e\nu} = 0.07 \pm 0.12$ for the electron-neutrino correlation. The lepton-plane correlation with the Λ spin, $D = 0.11 \pm 0.20$, is consistent with no violation of time-reversal invariance. Our data yield an axial-vector-to-vector form-factor ratio of $g_1/f_1 = 0.53^{+0.11}_{-0.09}$. The Cabibbo-model value is $g_1/f_1 = 0.71$.

I. INTRODUCTION

This paper describes an experiment carried out at the Argonne National Laboratory Zero Gradient Synchrotron to study the β decay of polarized Λ hyperons $\Lambda \to p + e + \bar{\nu}$. Polarized Λ's were produced in a liquid hydrogen target by the reaction $\pi^- p \to \Lambda K^0$ at 1025 MeV/c, just below ΣK threshold. The experiment employed optical spark chambers and counters in a magnetic spectrometer. β decays were identified by a combination of Cherenkov detector, time-of-flight, and kinematic techniques. This experiment was specifically designed to measure the angular correlations of the β-decay products with the Λ spin, to determine the electron-neutrino correlation, and to test for time-reversal invariance. In particular, the spin correlations are determined without significant bias. Momentum analysis of the Λ-decay products permits us to directly obtain all three spin correlations in the laboratory and to reconstruct the events in the rest frame of the Λ.

In the decay $A \to Be\bar{\nu}$, where A and B are the initial- and final-state baryons, the general vector-plus-axial-vector matrix element takes the form

$$M = \langle B | V_\alpha + A_\alpha | A \rangle \, \bar{e} i \gamma_\alpha (1 + \gamma_5) \nu \, . \tag{1}$$

Expanding the baryon matrix element, and discarding very small terms proportional to the electron mass, we obtain:

$$\begin{aligned} \langle B | V_\alpha | A \rangle &= i \bar{U}_B \left(\gamma_\alpha f_1(q^2) + \sigma_{\alpha\beta} \frac{q_\beta}{M_A} f_2(q^2) \right) U_A \, , \\ \langle B | A_\alpha | A \rangle &= i \bar{U}_B \left(\gamma_\alpha \gamma_5 g_1(q^2) + \sigma_{\alpha\beta} \frac{q_\beta}{M_A} \gamma_5 g_2(q^2) \right) U_A \, . \end{aligned} \tag{2}$$

Here, U_A and U_B are free Dirac spinors, and the form factors f_1 (vector), f_2 (weak magnetism), g_1 (axial vector), and g_2 (induced pseudotensor) are functions of the square of the four-momentum transfer $q = p_A - p_B = p_e + p_\nu$. The Cabibbo model[1] gives the form factors for all the leptonic decays of the octet baryons in terms of three parameters: the reduced axial-vector form factors F and D and the Cabibbo angle θ. The most recent conventional fit[2] to available baryon leptonic decay data gave

$$\begin{aligned} \theta &= 0.239 \, , \\ F &= 0.451 \, , \\ D &= 0.777 \, . \end{aligned} \tag{3}$$

The predicted form-factor ratios for Λ β decay are then

$$\begin{aligned} g_1/f_1 &= 0.71 \, , \\ f_2/f_1 &= 0.98 \, . \end{aligned} \tag{4}$$

Making the conventional assumptions $g_2 = 0$ and no violation of time-reversal invariance, these form-factor ratios, taken at face value, imply the following for the electron-neutrino correlation and the spin correlations[3] in Λ β decay:

$$\begin{aligned} A_{e\nu} &= -0.04 \, , \\ A_p &= -0.59 \, , \\ A_e &= 0.02 \, , \\ A_\nu &= 0.97 \, . \end{aligned} \tag{5}$$

Experimentally, the electron-neutrino correlation has been well determined by investigations of unpolarized decays and is in good agreement with the model. The spin correlations offer the advantage of sensitivity to phase, thus imposing many more

constraints on the space-time structure of the interaction. Their measurement, however, is considerably more challenging because either polarized initial baryons or polarization analysis of the final-state baryons is required. The present measurement represents the first *direct* determination of *both* types of correlations in a *single* experiment.

II. METHOD AND APPARATUS

A. Synopsis

The reaction $\pi^- p \to \Lambda K^0$ in hydrogen below ΣK threshold provides a source of highly polarized Λ's unencumbered by competing associated production channels. Magnetic analysis of the Λ-decay products combined with particle identification provides adequate information for measuring both the electron-neutrino correlation and the spin correlations, and for reconstructing the Λ rest frame. It is significant that detecting the K^0 decays is not required as this would reduce the number of detected Λ β decays by at least one order of magnitude.

The detection system was designed to measure the spin asymmetries without significant bias. This entailed symmetric detection efficiency with respect to the midplane of the apparatus, collection of nearly all protons from Λ decays (hence, no bias on the neutrinos), and efficient detection of all electrons within the acceptance of the electron Cherenkov counter.

B. Pion beam

A plan view of the secondary pion beam[4] is shown in Fig. 1. The external proton beam was focused onto a beryllium production target. Secondary particles were momentum selected and imaged onto a liquid hydrogen target by a two-stage configuration of magnets. The central momentum of the beam was 1025 ± 3 MeV/c. The momentum was determined in three ways: First by the wire-orbit technique; then in a positive beam by measurement of the time-of-flight separation between pions, protons, and deuterons; and finally, by measurement of deuteron range in aluminum. This gave three independent measurements of the beam momentum, which agreed within their standard deviations of $\pm 0.5\%$. A collimator placed between the two bending magnets set the momentum interval at ± 12 MeV/c. The composition of the secondary beam was 75% π^-, 22% e^-, and 3% μ^-. Electrons in the beam were vetoed by CO_2 Cherenkov counter C_1 (in Fig. 2) placed inside the last quadrupole. The typical instantaneous beam rate during data taking was 1 MHz.

C. Magnetic spectrometer

A plan view of our spectrometer is shown in Fig. 2. The analyzing magnet had pole faces measuring 0.5 m by 1 m and a 1-m gap.[5] The magnetic field at the center was 5.7 kG. The vertical component of the field was determined by moving a wire coil through the field volume in precisely known steps and measuring the integral of the voltage induced in the coil during each step. The resulting map of field differences was then combined with absolute measurements of the field at selected points to produce a map of the vertical component. The other two components were obtained analytically from a model in which field sources were represented by uniformly charged rectangles of judiciously chosen sizes, strengths, orientations, and positions.[6]

The liquid hydrogen target was a cylinder 2.5 cm in diameter by 36 cm long. Its vacuum jacket was a plastic scintillator (T) enabling us to form an effective "neutrals" coincidence ($\overline{C}_1 \cdot B_1 \cdot B_2 \cdot B_3 \cdot \overline{B}_4 \cdot \overline{T}$). This signature was consistent with charge exchange in hydrogen, or with associated production followed by either decay into neutrals or escape from the target prior to decay into charged particles.

It was necessary that our spectrometer simultaneously analyze high-momentum protons and low-momentum negative particles with comparable precision. This was accomplished by employing the full $\int B\,d1$ to bend the protons while the negative decay products were momentum analyzed in the fringe field of the magnet.

After traversing the fringe field, the negative particles passed through a six-element hodoscope (E) before entering a large phase-space acceptance gas Cherenkov counter (C_2).[7] Mirrors inside C_2 divided it into four optically indpendent quadrants. Tests at the University of Chicago Synchrocyclotron

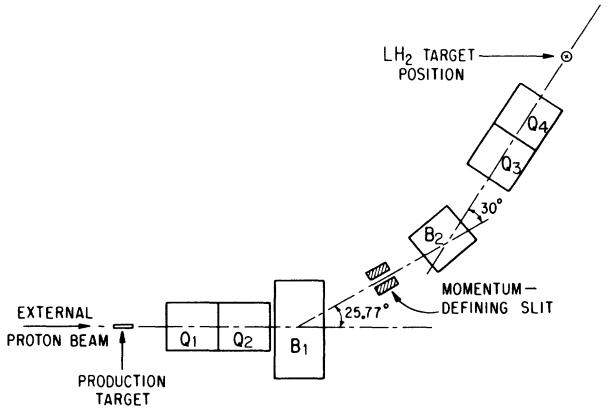

FIG. 1. Plan view of the secondary pion beam. Magnets Q_1, Q_2, Q_3, and Q_4 are quadrupoles; B_1 and B_2 are bending magnets.

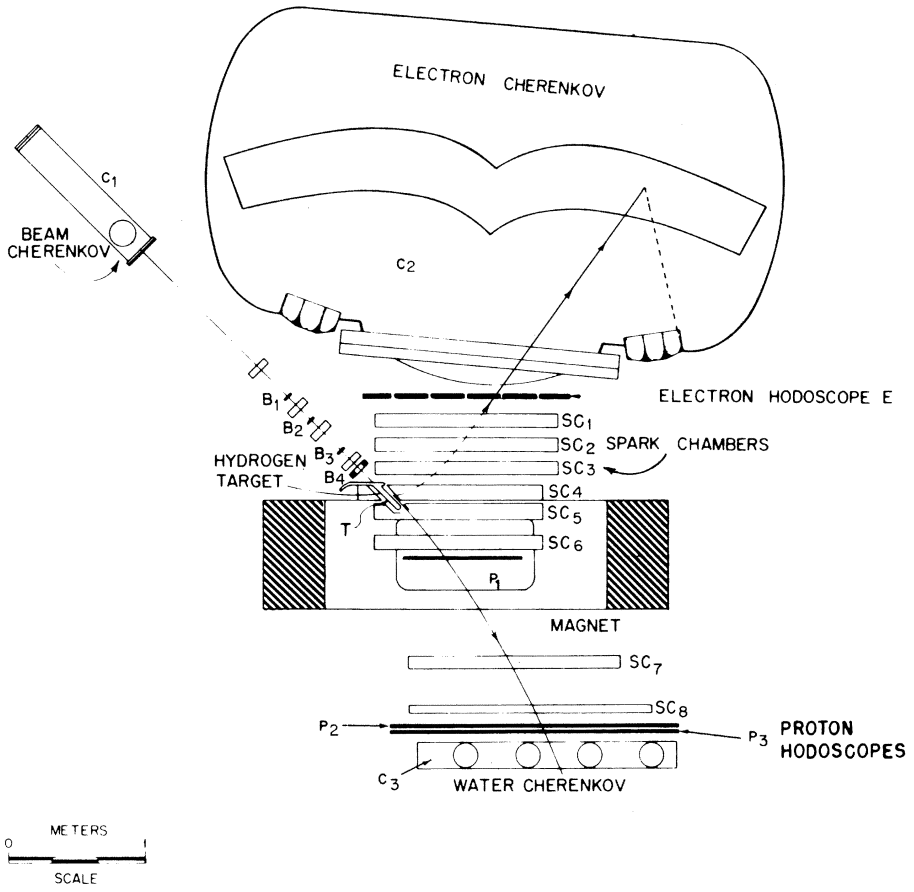

FIG. 2. Plan view of the experimental apparatus.

showed C_2 had an efficiency greater than 95% for electrons, and a scintillation efficiency for slow particles of less than 10^{-3}. The coincidence $(E \cdot C_2)$ defined an "electron" signal.

Protons from Λ decays entered the main field of the magnet, traversed the P_1 scintillator at the center of the magnet, and then two seven-element hodoscopes P_2 and P_3. A water-filled Cherenkov counter (C_2) was used to veto fast particles (π^+, e^+). It was viewed by 16 Amperex 58 AVP phototubes. Due primarily to scintillation, C_3 had a single-tube efficiency for protons from Λ decay of about 16%. By requiring at least two phototube signals from C_3, we reduced the slow-particle efficiency to less than 3%. A "proton" signal was formed from the coincidence $(P_1 \cdot P_2 \cdot P_3 \cdot \overline{C}_3)$.

The trigger for Λ β decay events was (neutral)(proton)(electron). To collect $\Lambda \to p\pi$ events, we simply switched the C_2 requirement out of the electron coincidence.

The trajectories of the charged decay products were sampled by eight thin-plate optical spark chambers and photographed in 90° stereo by two 35-mm Flight Research cameras. Incident beam particles were also observed with four small thin-plate chambers. Rows of fiducials at 5-cm intervals along the edges of the chambers obviated the effects of possible large-scale optical distortions and aided scanning by outlining the chambers on the film. The demagnification of the spark-chamber images on the film was typically 75. Our precision of reconstructing spark coordinates was determined using beam tracks and cosmic rays with the magnet turned off (straight line trajectories) and was found to be ±0.3 mm. A data box, photographed with both views of the chambers, displayed frame and run numbers and code lights identifying the elements of E and P_3 which contributed to the trigger. Another light tagged those triggers which were accompanied by a single phototube signal from C_3 ("$C_3 - 1$" triggers).

Decay product times of flight were recorded using two four-trace oscilloscope tubes.[8] Discriminator pulses from phototubes at the ends of the E and P_2 hodoscope elements were displayed on seven of the traces. The remaining trace showed the discrim-

inator output from the C_2 counter as well as the raw phototube signals from each C_2 quadrant. A timing reference marker at the beginning of each trace was derived from the output of the B_2 counter. The sweep speed was calibrated by photographing a 50-mHz sine wave every 100 frames, while delays in phototubes and cables were measured using e^+e^- pairs and $\Lambda p\pi$ events as sources of particles with known velocities.

Our data were accumulated during several running periods, each of about six weeks duration. Short $\Lambda \to p\pi$ runs alternated with $\Lambda \to pe\bar{\nu}$ runs at eight-hour intervals. At the end of each running period, data on πp scattering, beam tracks, and cosmic rays were taken to check spark-chamber alignment.

Data were also taken with the target emptied of hydrogen, and with the beam momentum below associated production threshold to provide information on possible sources of background.

III. DATA ANALYSIS

A. Selecting event candidates

The first stage of the data reduction process was a scan of the spark-chamber film. Scanners were instructed to look for "vees" with apparent vertices between chambers SC_3 and SC_6. Each particle was required to have the correct sign of curvature (electric charge). Scanning masks were used to verify that each particle entered the hodoscope elements specified by the data box. About 16% of the triggers contained such a vee. Most of these were electron-positron pairs with positron momenta well below the minimum (350 MeV/c) for a proton from Λ decay. By measuring the angle between the sparks in SC_6 and those in SC_7, the scanners could determine these low positive-particle momenta with a precision of ±40 MeV/c. All $C_3 - 1$ triggers with a positive momentum of less than 250 MeV/c were thus rejected. Scanners then performed simple measurements of the arc length for the positive-particle trajectory to the P_2 plane; this was prerequisite to interpreting the time-of-flight data. All frames in which no acceptable vee was found were rescanned, resulting in an over-all scanning efficiency greater than 96%.

Time-of-flight information for the vees was obtained by measuring the positions of pulses on the appropriate oscilloscope traces. The arithmetic average of the times measured for the tubes at both ends of a hodoscope element gave the particle time of flight with a precision of ±1.3 nsec. The difference between the two times was used to compute the point of impact of the particle along the hodoscope element. We later required this to agree with the reconstructed position to within ±10 cm.

Any vee whose positive-particle time-of-flight fell within 1.5 nsec of a positron ($v/c = 1$) flight time as calculated from the approximate path length was rejected. Since the *minimum* proton-positron time-of-flight separation for a Λ event is 3 ns, this cut, which rejected 75% of the vees, caused a negligible loss of good events. To suppress background caused by randoms or scintillation light in C_2, we imposed two consistency conditions on the C_2 signals: (a) that the quadrant match the trajectory extrapolated to the mirror, and (b) that the measured time of flight be correct to ±4 ns.

The spark-chamber film for vees surviving these cuts was examined to verify the initial identification, and the spark coordinates were digitized using measuring machines with a least count corresponding to 75 μm in real space.

Beam orbits, vertex positions, and decay-product momenta were reconstructed using an iterative fitting procedure[6] in which the decay products were assumed to come from a common vertex. This procedure included corrections for multiple Coulomb scattering, energy loss, and spark staggering.

In this experiment, a neutral particle (K^0 or Λ) decaying in a two-body mode could be kinematically reconstructed with three constraints. We chose to parametrize these with the invariant mass of the vee, the missing mass at the production vertex, and the total momentum transverse to the production plane. Our reconstructed vees were subjected to this analysis using all allowable assumptions on decay-particle types. In case a candidate showed more than one track in the beam chambers, scanning masks were used to reject noninteracting tracks or tracks intersecting the B_4 counter; about half of the triggers showed multiple beam tracks. Candidates were then classified according to the criteria given in Table I. In cases where a vee

TABLE I. Candidate classification.

Type	Criteria
	(A) Event candidates
$\Lambda \to pe\bar{\nu}$	Both proton and electron identified; the negative track has no kink; no extra tracks emanate from decay vertex region; the fitted decay vertex is outside T. The final separation into $\Lambda\beta$ and $\Lambda p\pi$ decays is performed on the basis of a χ^2 test (see text).
	(B) Identified backgrounds
e^+e^- pair	$M(e^+e^-) \leq 100$ MeV/c^2, correct positron time of flight to 3 nsec.
$K_L^0 \to \pi^+e^-\bar{\nu}$	$M(e^+e^-) > 100$ MeV/c^2, decay length >18 cm, correct π^+ time of flight to 3 nsec.

was associated with time-of-flight information inconsistent with any particle hypothesis or with pulse pair separations inconsistent with the reconstructed orbits, the oscilloscope film was remeasured. If the inconsistency persisted, the frame was rejected. A final scan of the spark-chamber film rejected any vee which had more than two tracks coming from the region of the decay vertex.

B. Identifying the event sample

At this stage of the analysis our data sample consisted of 771 $\Lambda \to pe\bar{\nu}$ candidates. A series of critical tests detailed below convinced us that this large sample consisted of an approximately equal mixture of $\Lambda \to pe\bar{\nu}$ and $\Lambda \to p\pi$ decays undiluted with any other significant background. To reduce the $\Lambda \to p\pi$ content, we used the three constraints already discussed to form a χ^2:

$$\chi^2 = \left(\frac{M_\Lambda^* - M_\Lambda}{\sigma_{M_\Lambda}}\right)^2 + \left(\frac{P_t}{\sigma_{P_t}}\right)^2 + \left(\frac{M_K^* - M_K}{\sigma_{M_K}}\right)^2 , \qquad (6)$$

where starred values are those reconstructed for each event. The standard deviations of the three quantities were measured using $\Lambda p\pi$ events. Background from $\Lambda p\pi$ decays was eliminated by rejecting candidates with a χ^2 less than some specific value. We calibrated the effect of this procedure on $\Lambda p\pi$ events with our $\Lambda p\pi$ data, and its effect on $\Lambda\beta$ events using a Monte Carlo simulation. It was therefore *not* necessary for us to assume that this quantity had a χ^2 distribution, and our results are *not* sensitive to the modest correlations between the three quantities.

By varying the location of the χ^2 cut, we could prepare event samples with different $\Lambda p\pi$ contaminations. Our calculations of the $\Lambda p\pi$ content in each sample are confirmed by the fact that we can correct the spin asymmetries and electron-neutrino correlation at all values of the $\Lambda p\pi$ contamination to give results that are in reasonable agreement. The stability of our results with respect to $\Lambda p\pi$ contamination is shown in Fig. 3.

Our physics results are based on a sample of 441 events with a $\Lambda p\pi$ χ^2 greater than 20 and a $\Lambda p\pi$ background of 13.8%. An additional 62 events were used in the branching-ratio determination but, due to large errors in the reconstruction of the Λ production point, were not included in our other results. There are also 41 events with multiple beam tracks in which we were unable to reliably select the correct pion by our visual technique.

The average Λ polarization for our data was measured using a sample of 3176 single-beam pion $\Lambda p\pi$ events. Taking the value 0.647 ± 0.013 for the proton asymmetry parameter α in $\Lambda p\pi$ decay,[9] the proton asymmetry for this event sample gives a polarization $P_\Lambda = 0.78 \pm 0.04$. We can also obtain a sample of $\Lambda p\pi$ events from our 771 $\Lambda\beta$ candidates by selecting only those events which have a $\Lambda p\pi$ χ^2 less than 10 and hence fit a $\Lambda p\pi$ hypothesis. This sample of 268 events gives a polarization of 0.86 ± 0.16. This demonstrates that the C_2 requirement does not bias the $\Lambda p\pi$ events observed in $\Lambda\beta$ triggers, again confirming our procedure for correcting the $\Lambda\beta$ decay correlations for $\Lambda p\pi$ background.

Our sample of $\Lambda p\pi$ events also provides the normalization for our determination of the branching ratio $\Lambda\beta$/all Λ. Taking $\Lambda p\pi$/all $\Lambda = 0.642$,[9] we obtain a value

$$\Lambda\beta/\text{all } \Lambda = (0.79 \pm 0.07) \times 10^{-3} . \qquad (7)$$

This is in agreement with the present world average[9] of $(0.813 \pm 0.029) \times 10^{-3}$. Moreover, the average center-of-mass lifetime of the $\Lambda\beta$ events is 0.65 ± 0.02 nsec in agreement with the corresponding value determined for our $\Lambda\pi p$ events (0.60 ± 0.02 nsec). The shape of the two lifetime distributions are also in excellent agreement (Fig. 4). Clearly these characteristics of the data support the absence of any significant non-Λ background. However, we further applied a series of critical tests to gain additional confidence that the data sample was free of background and systematic effects.

C. Backgrounds and systematics

We have subjected our data to a series of tests designed to uncover possible sources of nonrandom error. For most of these, the critical property evaluated was the sensitivity of the asymmetries to a sequence of cuts on a particular laboratory

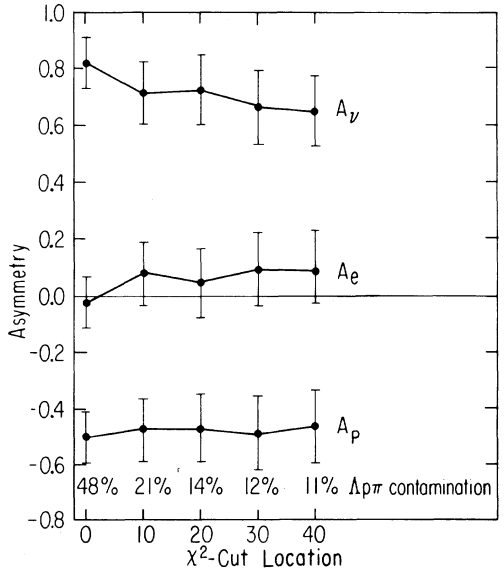

FIG. 3. Spin asymmetries as a function of $\Lambda p\pi$ contamination.

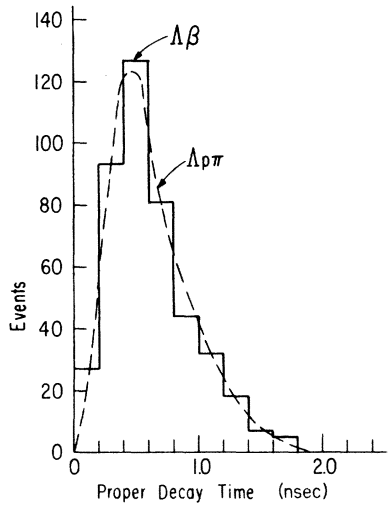

FIG. 4. Λ proper-lifetime distributions. Note that the distribution shape is biased by the requirement that all Λ's escape from the T counter.

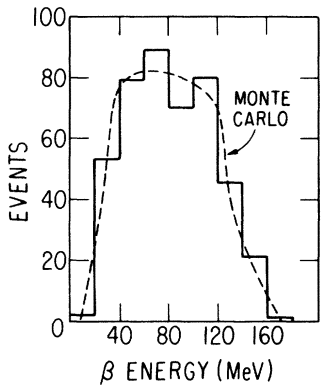

FIG. 5. Center-of-mass β spectrum.

quantity. The results of these tests are summarized in Table II. We note that the asymmetries are given without correction for $\Lambda p\pi$ background, or in the case of the electron-neutrino correlation, for bias induced by the apparatus. Each type of selection was motivated by a hypothetical source of nonrandom error as follows.

1. Bias induced by the apparatus

A set of 4000 fully triggered Monte Carlo events showed that at this level of statistical precision the spin asymmetries of the detected events are the same as those of the decays themselves. Another set of 4000 Monte Carlo $\Lambda p\pi$ events showed the same to be true of $\Lambda p\pi$ data. Pairs, π-p scatters, and $\Lambda p\pi$ events have been used to demonstrate that the up-down asymmetry for particle detection in our apparatus is less than 0.03. Furthermore, we have divided our sample of $\Lambda\beta$ events into two sets according to whether the Λ spin points up or down in the laboratory and find no statistically significant difference between the asymmetries of the two samples (Table II, entry 2).

Although the electron detection efficiency of the C_2 counter was measured to be greater than 95% over the whole of the phase space accepted by the counter, we isolated the subsample of events in the region where the efficiency is expected to be greater than 99% and find that the asymmetries agree well with those of the full sample (Table II, entry 3). We also find that the fraction of the events lying within this region of phase space agrees well with the fraction of the Monte Carlo events in the same region, suggesting that the 95% value for the minimum electron efficiency is an underestimate. Our experimental β spectrum is shown in Fig. 5. The biases are geometric in origin and well represented by the Monte Carlo.

TABLE II. Event subsamples and asymmetries.

Sample	Events	A_p	A_e	A_ν	A_ν
Standard event sample	441	−0.32 ± 0.13	0.04 ± 0.13	0.71 ± 0.13	−0.13 ± 0.10
Λ spin up only	173	−0.26 ± 0.19	−0.13 ± 0.19	0.47 ± 0.19	−0.22 ± 0.15
Cherenkov counter phase-space cut	318	−0.31 ± 0.14	0.01 ± 0.14	0.69 ± 0.14	−0.03 ± 0.11
Single-beam-pion events only	217	−0.40 ± 0.18	0.09 ± 0.18	0.81 ± 0.18	−0.19 ± 0.14
Minimum vertex-pion distance greater than 1.2 cm	381	−0.35 ± 0.13	−0.03 ± 0.13	0.77 ± 0.13	−0.14 ± 0.10
Decay vertex more than 2.5 mm from T	218	−0.29 ± 0.18	0.09 ± 0.18	0.67 ± 0.18	0.08 ± 0.14
Positive extrapolation less than 10 cm	241	−0.32 ± 0.17	0.04 ± 0.17	0.62 ± 0.17	−0.08 ± 0.13
Hydrogen-produced events only	231	−0.41 ± 0.17	0.10 ± 0.17	0.71 ± 0.17	0.02 ± 0.13
Kinematic failures only	137	−0.23 ± 0.22	−0.17 ± 0.22	0.64 ± 0.22	−0.11 ± 0.17

2. Event systematics

We consider our visual procedure for choosing the correct beam pion in triggers showing more than one track in the beam chambers to be thoroughly reliable. To verify this, we isolated those events which had only one track in the beam chambers and looked at the asymmetries of this subsample (Table II, entry 4). We find that these asymmetries are consistent with the values for the full sample. For some events the distance of closest approach between the pion orbit and the Λ-decay vertex was small. In these events it was possible for errors in the reconstruction of the decay vertex position to cause the production plane to be poorly determined. To see if this affected our results, we removed from the sample all events which have distances of closest approach less than 12 mm (compared to our vertex reconstruction precision of about 13 mm) (Table II, entry 5). We find that removing these events causes no statistically significant change in the asymmetries.

It is possible that some decays originated in a "skin" on the outer surface of T without generating enough scintillation light to efficiently veto. Interactions of the decay products with the scintillator would perhaps wash out the asymmetries. We isolated those events which had reconstructed decay vertices greater than 2.5 mm from the nearest part of T and examined their asymmetries (Table II, entry 6). We again find them to be consistent with those of the full sample. For certain events, the distance of extrapolation from the decay vertex to the first measured spark could be quite long—in excess of 10 cm, for example. Excluding these events from the data has no significant effect on the relevant quantities (Table II, entry 7). Data taken with the target emptied of hydrogen showed that about 15% of our Λ's were produced in T itself. To evaluate this effect, we isolated events which could be identified as necessarily produced in hydrogen. We did this by calculating for each event the point where the extrapolated pion orbit would have left the hydrogen volume if the pion had not interacted, and then computed what the beam-Λ angle would have been if this had been the production point. Examination of the $\Lambda p\pi$ events produced in scintillator showed that the maximum beam-Λ angle for events produced in carbon is about 30°, and so by requiring the hypothetical production angle to be greater than 45° we could prepare a sample of events which could only have been produced in hydrogen (Table II, entry 8). These events had asymmetries in statistical agreement with those of the full sample.

Our zero-constraint kinematics for $\Lambda \to pe\bar{\nu}$ lead to a quadratic equation for the laboratory Λ momentum and hence to a two-solution ambiguity in the transformation to the Λ rest frame. To deal with this, we formed a weight for each solution from the product of the probabilities of the Λ production angle and the center-of-mass Λ lifetime. By rejecting solutions corresponding to Λ production outside the target we rejected unphysical solutions. Normalizing the sum of the probabilities to 1 assigned the solutions proper relative weights. About 30% of our events failed to reconstruct zero-constraint kinematics. This occurred when measuring errors caused the discriminant of the quadratic equation for the Λ momentum to become negative. By "stretching" the neutrino momentum to the nearest kinematically allowed value in the particular frame where the sum of the momenta of the charged-decay products is purely transverse, we were able to assign a unique center-of-mass solution to these events. These stretched events were examined with respect to biasing the asymmetries. No such effect is visible (Table II, entry 9).

3. Non-Λ background

We examined the possibility that some of the events in our data sample were not from Λ decays. One important check of this is a sample of data taken with the pion beam momentum set to 850 MeV/c, which is below the threshold for Λ production, but in a region where the charge-exchange cross section is still large. We took sufficient data at this momentum to have generated 28 $\Lambda\beta$ events at nominal beam momentum and found no acceptable candidates. The e^+e^- invariant mass of pairs peaks very sharply below 100 MeV, and a significant contamination of our sample by pairs would thus result in an excess of events with low pair masses. Figure 6 shows the e^+e^- invariant mass of our event sample, along with the distribution predicted by Monte Carlo. The dotted histogram shows the e^+e^- invariant-mass distribution for pairs in our apparatus, normalized to 10% of the $\Lambda\beta$ sample and added to the $\Lambda\beta$ histogram to illus-

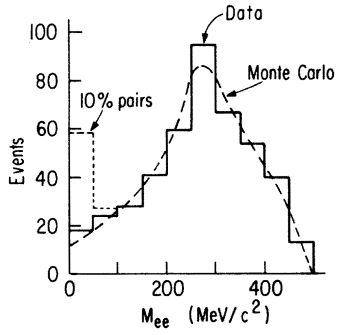

FIG. 6. Comparison of e^+e^- invariant-mass (M_{ee}) distributions.

trate the effect this much pair background would have on the distribution. No significant excess of low-mass events is seen.

Pions from kaon decays are eliminated by the C_3 anticoincidence counter and time of flight. To corroborate the absence of light positive particles in our data sample we have used the observation (deduced from $\Lambda p\pi$ events) that the single-tube efficiency of C_3 for protons from Λ decays is $(16 \pm 1)\%$. In contrast, over 65% of all triggers identified as pairs were accompanied by a single-tube signal from C_3. In our $\Lambda\beta$ data sample we find that $(15 \pm 2)\%$ of our events have a single-tube signal from C_3, confirming the absence of any significant background of fast positive particles in our data.

IV. RESULTS AND CONCLUSIONS

Preliminary results based on the first third of the data sample were presented in Ref. 10.

Our final values for the correlations of the decay proton, electron, and neutrino with the Λ spin, corrected for $\Lambda p\pi$ background are

$$A_P = -0.47 \pm 0.12\,,$$
$$A_e = 0.05 \pm 0.12\,, \tag{8}$$
$$A_\nu = 0.72 \pm 0.12\,.$$

Figure 7 shows the neutrino angular distribution in the Λ rest frame.

A nonzero value for the correlation between the lepton plane and the Λ spin, proportional to $\vec{P}_\Lambda \cdot(\hat{e}\times\hat{\nu})$, would indicate a violation of time-reversal invariance. We have evaluated this asymmetry directly in the Λ rest frame and find

$$D = 0.11^{+0.19}_{-0.20} \tag{9}$$

consistent with no violation. This corresponds to a phase difference between the vector and axial-vector currents of

$$\phi = -(15^{+28}_{-30})^\circ\,. \tag{10}$$

We therefore make the conventional assumption $\phi = 0$ in our subsequent analysis.[11]

We have also performed a maximum-likelihood analysis of the Dalitz plot in the Λ rest frame. This gives the electron-neutrino correlation which can be directly compared with existing data on decays of unpolarized Λ's. A correction for the variation of f_1 and g_1 with the momentum transfer between the Λ and the proton was made in the fit, assuming the variation to be

$$f_1(q^2) = f_1(0)/(1 - q^2/M_V{}^2)^2\,,$$
$$g_1(q^2) = g_1(0)/(1 - q^2/M_A{}^2)^2\,. \tag{11}$$

We used the values[12] $M_V = 0.84$ GeV/c^2 and $M_A = 0.89$ GeV/c^2. An additional correction was made for

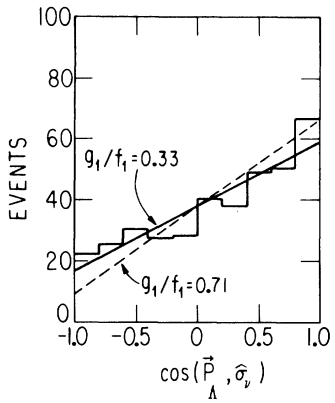

FIG. 7. Center-of-mass neutrino-spin cosine distribution.

radiative distortion[13] of the shape of the electron-energy spectrum. Taking $g_2 = 0$, the likelihood was found to maximize at $|g_1/f_1| = 0.60^{+0.13}_{-0.10}$ and $f_2/f_1 = 0.4^{+0.8}_{-0.7}$, which corresponds to

$$A_{e\nu} = 0.07 \pm 0.12\,. \tag{12}$$

Previous analysis of $\Lambda \to pe\bar{\nu}$ experimental data have ignored the q^2 dependence of f_1 and g_1. A Dalitz-plot fit in which this was done gave a likelihood maximum at

$$|g_1/f_1| = 0.68^{+0.14}_{-0.11} \text{ and } f_2/f_1 = 0.6^{+0.8}_{-0.7}\,. \tag{13}$$

Our result for the electron-neutrino correlation is in excellent agreement with existing experimental data (see Table III) and with the value given by the Cabibbo model.

Since the value of f_2/f_1 is most directly obtained from the Dalitz plot, and our value agrees with the predictions of the octet extension of the conserved-vector-current hypothesis ($f_2/f_1 = 0.98$), we adopt this value. A simultaneous fit to $A_{e\nu}$ and the three statistically independent asymmetry sums $(A_e + A_p)$, $(A_p + A_\nu)$, $(A_e + A_\nu)$ then gives $g_1/f_1 = 0.53^{+0.11}_{-0.09}$. The χ^2 is 2.74 for three degress of freedom with a 43% confidence level. An analysis of the spin-asymmetry sums alone yields $g_1/f_1 = 0.33^{+0.14}_{-0.09}$. These results clearly verify the general $V-A$ nature of the $\Lambda\beta$ matrix element predicted by the Cabibbo model, but they suggest a smaller value than the $g_1/f_1 = 0.71$ obtained in conventional fits[2] to the model.

Comparing our data with other experiments[14-23] (see Table III), we find that all experiments which measure spin correlations are in clear agreement. The electron-neutrino correlation obtained in our experiment also agrees with a recent bubble-chamber result[14] and with older data. We therefore average the measured angular correlations to obtain the weighted means given in Table III. The three spin-correlation sums yield $g_1/f_1 = 0.42^{+0.09}_{-0.07}$

TABLE III. Summary of experimental results on $\Lambda \rightarrow pe\bar{\nu}$.

Experiment	Events Total	Events Analyzed	Polarization	A_ν	A_e	A_p	$A_{e\nu}$	$10^3 \times$ Branching ratio
This experiment	544	441	0.78 ± 0.04	0.72 ± 0.12	0.05 ± 0.12	−0.47 ± 0.12	0.07 ± 0.12	0.79 ± 0.07
Maryland[a]	1075	645					0.01 ± 0.07	0.817 ± 0.044
CERN-Heidelberg[b]	1078	817	0.75 ± 0.03	0.89 ± 0.08	0.15 ± 0.09	−0.51 ± 0.09	0.07 ± 0.085	0.84 ± 0.04
Burnett *et al.*[c]		405	0.70 ± 0.02	0.75 ± 0.15	d	−0.56 ± 0.15	0.16 ± 0.13	
Baggett *et al.*[e]	416	352					0.00 ± 0.08	
Carnegie-Mellon[f]		271					0.10 ± 0.13	
Canter *et al.*[g]	198	141					0.00 ± 0.14	0.78 ± 0.09
Baglin *et al.*[h]		102					−0.21 ± 0.24	0.75 ± 0.12[i]
Barlow *et al.*[j]		84	0.60 ± 0.10		0.06 ± 0.19			
Ely *et al.*[k]	150	59					< 0.05[l]	0.79 ± 0.13[i]
Lind *et al.*[m]		22	0.91 ± 0.10	0.74 ± 0.39	0.60 ± 0.35		−0.06 ± 0.34	1.49 ± 0.33[i,l]
Weighted mean				0.821 ± 0.060	0.125 ± 0.066	−0.508 ± 0.065	0.036 ± 0.037	0.816 ± 0.026
Consistency χ^2/degree of freedom				1.7/3	2.4/3	0.2/2	2.9/8	1.0/5

[a] Reference 14.
[b] Reference 15.
[c] Reference 16.
[d] No value quoted owing to uncertainties in experimental biases.
[e] Reference 17.
[f] Reference 18.
[g] Reference 19.
[h] Reference 20.
[i] Corrected for current value of $\Lambda p\pi$/all $\Lambda = 0.642 \pm 0.005$.
[j] Reference 21.
[k] Reference 22.
[l] Not included in weighted mean
[m] Reference 23.

compared to $g_1/f_1 = 0.628^{+0.038}_{-0.035}$ from A_{ev}. A combined fit to all four parameters gives $g_1/f_1 = 0.611^{+0.035}_{-0.033}$ with $\chi^2 = 5.42$ for three degress of freedom (probability 14%). It is apparent that the g_1/f_1 value from the spin asymmetries is smaller than that from A_{ev}, and that results from all polarized Λ experiments agree on this point. The mediocre χ^2 for the combined fit also reflects this dichotomy. An analogous χ^2 computation using the conventional Cabibbo form-factor values gives $\chi^2 = 7.44$ for four degrees of freedom (probability 11%).

These consistent differences could indicate some additional contribution to the decay matrix element not contained in the conventional analysis. One such possibility would be the presence of a g_2 term.[24] It is, of course, also possible that the experiments are subject to some common systematic problem; for example, an error in the determination of the $\Lambda \to p\pi$ asymmetry parameter[9,25] which sets the scale for the Λ polarization.

These questions aside, hyperon β-decay experiments, and particularly measurements on polarized $\Lambda \to pe\bar{\nu}$, have unambiguously established the relative sign of the vector and axial-vector interaction in strangeness-changing weak processes.[25] However, to definitively test the Cabibbo model,[26] and to explore the nature of symmetry breaking, additional high-statistics polarized hyperon β-decay experiments are needed.

ACKNOWLEDGMENTS

We are grateful to Argonne National Laboratory for its hospitality and for the vital support provided by the staff of the Zero Gradient Synchrotron. The scientific contributions of P. R. Phillips and the engineering contributions of C. J. Rush and J. Terandy were invaluable. Technical assistance from D. Burandt, E. Hayes, G. Karambis, L. Lavoie, B. Nelson, J. Tate, and J. Upton is gratefully acknowledged. We also thank our scanning and measuring personnel, particularly B. Stevens and C. Fineberg, for their efforts. We are indebted to S. Watson for her diligent help with the data processing.

---

*Work supported in part by the U. S. Energy Research and Development Administration and the National Science Foundation.

†Work submitted in partial fulfillment of the requirements for the degree of Ph.D. in physics at the University of Chicago.

‡Present address: Department of Physics, Elmhurst College, Elmhurst, Illinois 60126.

§Present address: Joseph Henry Laboratory, Princeton University, Princeton, New Jersey 08540.

||Present address: Argonne National Laboratory, Argonne, Illinois 60439.

¶Joint appointee at Argonne National Laboratory.

**Present address: Department of Physics and Astronomy, University of New Mexico, Albuquerque, New Mexico 87106.

††Present address: Zettler Software Company, Columbus, Ohio 43215.

‡‡Present address: Brookhaven National Laboratory, Upton, New York 11973.

[1]N. Cabibbo, Phys. Rev. Lett. 10, 531 (1963); also M. Gell-Mann and M. Levy, Nuovo Cimento 16, 705 (1960); and Z. Maki, M. Nakagawa, and S. Sakata, Prog. Theor. Phys. 28, 870 (1962).

[2]E. Ebenhoh, F. Eisele, H. Filthuth, W. Föhlisch, V. Hepp, E. Leitner, W. Presser, H. Schneider, T. Thouw, and G. Zech, Z. Phys. 241, 473 (1971).

[3]We define the spin-correlation parameters used in the text in the usual way: $A_i P_\Lambda = 2[N(i\uparrow) - N(i\downarrow)]/[N(i\uparrow) + N(i\downarrow)]$, where decay product i is $\uparrow$ or $\downarrow$ as the projection of its momentum along the polarization vector is positive or negative, respectively. Experimentally, we evaluate the A_i with the ratio-of-moments estimator: $A_i P_\Lambda = \langle \cos\theta_i \rangle / \langle \cos^2\theta_i \rangle$, where θ_i is the angle between P_Λ and the direction of decay product i. This is an efficient estimator which has the advantage that it cancels all symmetric biases.

[4]A. Stevens, D. Schwartz, C. Rush, K. Reibel, T. A. Romanowski, R. L. Sumner, E. Swallow, J. Watson, R. Winston, and D. Wolfe, Nucl. Instrum. Methods 87, 207 (1971).

[5]T. A. Romanowski, E. Hayes, J. Terandy, and K. Reibel, Nucl. Instrum. Methods 73, 117 (1969).

[6]P. R. Phillips, Nucl. Instrum. Methods 75, 71 (1969); also V. Highland and R. Macek, *ibid.* 64, 69 (1968).

[7]H. Hinterberger, L. Lavoie, B. Nelson, R. Sumner, J. Watson, R. Winston, and D. Wolfe, Rev. Sci. Instrum. 41, 413 (1970).

[8]R. Sumner, Nucl. Instrum. Methods 100, 371 (1972).

[9]Particle Data Group, Rev. Mod. Phys. 48, S1 (1976).

[10]J. Lindquist, R. L. Sumner, J. M. Watsor, R. Winston, D. M. Wolfe, P. R. Phillips, E. C. Swallow, K. Reibel, D. M. Schwartz, A. J. Stevens, and T. A. Romanowski, Phys. Rev. Lett. 27, 612 (1971).

[11]See A. Garcia, Phys. Rev. D 3, 2638 (1971); also J. M. Watson and R. Winston, Phys. Rev. 181, 1907 (1969). With our sign convention, $g_1/f_1 = +1.25$ for $n \to pe\bar{\nu}$. Throughout our analysis we take proper account of the coherent uncertainty in A_e, A_ν, and A_p due to the statistical uncertainty in our knowledge of the Λ polarization.

[12]W. A. Mann, U. Mehtani, B. Musgrave, Y. Oren, P. A. Schreiner, R. Singer, H. Yuta, R. Ammar, S. Barish, Y. Cho, M. Derrick, R. Engelmann, and L. G. Hyman, Phys. Rev. Lett. 31, 844 (1973).

[13]A. Sirlin, Phys. Rev. 164, 1767 (1967).

[14]C. N. Katz, Ph.D. thesis, University of Maryland Technical Report No. 74-044, 1973 (unpublished); also G. A. Snow (private communication).

[15]K. H. Althoff, R. M. Brown, D. Freytag, K. S. Heard,

J. Heintze, R. Mundhenke, H. Rieseberg, V. Soergel, H. Stelzer, and A. Wagner, Phys. Lett. 37B, 531 (1971); 37B, 535 (1971); 43B, 237 (1973). The full sample of 1078 events was employed in the direct laboratory determination of A_e, A_p, and the branching ratio, and in a Monte Carlo based analysis of a laboratory angular correlation to obtain $A_{e\nu}$. Time-of-flight data were used for the restricted sample of 817 events to estimate K^+ and p^+ momenta. A_ν was then obtained from this subsample by a detailed comparison with the Monte Carlo simulation.

[16]T. H. Burnett, W. Innes, G. Masek, T. Maung, E. S. Miller, H. Ruderman, J. Smith, and W. Vernon, Nuovo Cimento 34, 14 (1976); also T. H. Burnett (private communication).

[17]N. Baggett, M. Baggett, F. Eisele, H. Filthuth, H. Frehse, V. Hepp, R. Howard, E. Leitner, and G. Zech, Z. Phys. 249, 279 (1972).

[18]C. T. Murphy (private communication).

[19]J. Canter, J. Cole, J. Lee-Franzini, and R. J. Loveless, Phys. Rev. Lett. 26, 868 (1971).

[20]C. Baglin, V. Brisson, A. Rousset, J. Six, H. H. Bingham, M. Nikolic, K. Schultze, C. Henderson, D. J. Miller, F. R. Stannard, R. T. Elliot, L. K. Rangan, A. Haatuft, and K. Myklebost, Nuovo Cimento 35, 977 (1965).

[21]J. Barlow, I. M. Blair, G. Conforto, M. I. Ferrero, C. Rubbia, J. C. Sens, P. J. Duke, and A. K. Mann, Phys. Lett. 18, 64 (1965).

[22]R. P. Ely, G. Gidal, G. E. Kalmus, W. M. Powell, W. J. Singleton, C. Henderson, D. J. Miller, and F. R. Stannard, Phys. Rev. 137, B1302 (1965); 131, 868 (1963).

[23]V. G. Lind, T. O. Binford, M. L. Good, and D. Stern, Phys. Rev. 135, B1483 (1964).

[24]R. Oehme, R. Winston, and A. Garcia, Phys. Rev. D 3, 1618 (1971).

[25]R. Oehme, E. Swallow, and R. Winston, Phys. Rev. D 8, 2124 (1973).

[26]See A. Garcia and E. Swallow, Phys. Rev. Lett. 35, 467 (1975).